We are IntechOpen, the world's leading publisher of Open Access books Built by scientists, for scientists

6,900
Open access books available

185,000
International authors and editors

200M
Downloads

Our authors are among the

154
Countries delivered to

TOP 1%
most cited scientists

12.2%
Contributors from top 500 universities

WEB OF SCIENCE™

Selection of our books indexed in the Book Citation Index in Web of Science™ Core Collection (BKCI)

Interested in publishing with us?
Contact book.department@intechopen.com

Numbers displayed above are based on latest data collected.
For more information visit www.intechopen.com

2

SOAs Nonlinearities and Their Applications for Next Generation of Optical Networks

Youssef Said and Houria Rezig
Sys'Com Laboratory, National Engineering School of Tunis (ENIT)
Tunisia

1. Introduction

Semiconductor optical amplifiers (SOAs) have attracted a lot of interest because of their application potential in the field of optical communications. Their use has been envisaged in different applications in the access, core and metropolitan networks. Particularly, they have been envisioned for all-optical signal processing tasks at very high bit rates that cannot be handled by electronics, such as wavelength conversion, signal regeneration, optical switching as well as logic operations. To implement such all-optical processing features, the phenomena mostly used are: cross gain modulation (XGM), cross phase modulation (XPM), four-wave mixing (FWM) and cross polarization modulation (XPolM).

The aim of the present work is to present a qualitative and an exhaustive study of the nonlinear effects in the SOA structure and their applications to achieve important functions for next generation of optical networks. These phenomena are exploited in high speed optical communication networks to assure high speed devices and various applications, such as: wavelength converters in WDM networks, all-optical switches, optical logic gates, etc. Particularly, we focus on analyzing the impact of variation of intrinsic and extrinsic parameters of the SOA on the polarization rotation effect in the structure. This nonlinear behavior is investigated referring to numerical simulations using a numerical model that we developed based on the Coupled Mode Theory (CMT) and the formalism of Stokes. Consequently, it is shown that the azimuth and the ellipticity parameters of the output signal undergo changes according to injection conditions, i.e. by varying the operating wavelength, the input polarization state, the bias current, the confinement factor and obviously the SOA length, which plays an important role in the gain dynamics of the structure. We will show that the obtained results by the developed model are consistent with those obtained following the experimental measurements that have been carried out in free space.

In addition, an investigation of the impact of nonlinear effects on the SOA behavior in linear operating and saturation regimes will be reported. Their exploitation feasibility for applications in high bit rate optical networks are therefore discussed. Hence, the impact of variation of the SOA parameters on the saturation phenomena is analyzed by our numerical simulations. It was shown that high saturation power feature, which is particularly required in wavelength division multiplexing (WDM) applications to avoid crosstalk arising from gain saturation effects, can be achieved by choosing moderate values of the operating parameters. Moreover, we will address one of the essential processes to consider in SOAs

analysis, which is the noise. Particularly, we numerically simulate the impact of noise effects on the SOA behavior by measuring the gain, the optical signal to noise ratio and the noise figure. Although its gain dynamics provide very attractive features of high speed optical signal processing, we show that the noise is important in SOAs and can limit the performance of the structure. In order to remedy this, we show that using high bias current at moderate input signal power is recommended.

We report and characterize the impact of the nonlinear polarization rotation on the behavior of a wavelength converter based on XGM effect in a SOA at 40 Gbit/s. Moreover, we investigate and evaluate its performance as function of the intrinsic and extrinsic SOA parameters, such as the bias current, the signal format, the input signal power and its polarization state that determine the magnitude of the polarization rotation by measuring the ellipticity and the azimuth. Also, the impact of noise effects on the structure behavior is investigated through determining the noise figure. In particular, we focus on the performance of an improved wavelength conversion system via the analysis of quality factor and bit error rate referring to numerical simulation.

In this chapter, we deal either with the investigation of the SOA nonlinearities; particularly those are related to the polarization rotation, to exploit them to assure important optical functions for high bit rate optical networks. The dependence of SOA on the polarization of the light is an intrinsic feature which can lead to the deterioration of its performance. As a system, it is very inconvenient because of the impossibility to control the light polarization state, which evolves in a random way during the distribution in the optical fiber communication networks. For that reason, the technological efforts of the designers were essentially deployed in the minimization of the residual polarimetric anisotropy of the SOAs, through the development of almost insensitive polarization structures. On the other hand, various current studies have exploited the polarization concept to assure and optimize some very interesting optical functions for the future generation of the optical networks, as the wavelength converters, the optical regenerators and the optical logical gates. In this frame, many studies have demonstrated, by exploiting the nonlinear polarization rotation, the feasibility of the implementation of optical logical gates, wavelength converters and 2R optical regenerators.

2. Semiconductor optical amplifier: Concept and state of the art

2.1 SOA architecture

A semiconductor optical amplifier (SOA) is an optoelectronic component, which is characterized by a unidirectional or bidirectional access. Its basic structure, represented in figure 1, is slightly different from that of the laser diode. Indeed, there will be creation of the following effects: the inversion of population due to the electric current injection, the spontaneous and stimulated emission, the non-radiative recombination. Contrary to semiconductor lasers, there are no mirrors in their extremities but an antireflection coating, angled or window facet structures have been adopted to reduce light reflections into the circuit. SOAs manufacturing is generally made with III-V alloys, such as the gallium arsenide (GaAs), indium phosphide (InP) and various combinations of these elements according to the required band gap and the characteristics of the crystal lattice. In particular case for use around 1,55 μm, the couple InGaAsP and InP is usually used for the active layer and the substratum, respectively.

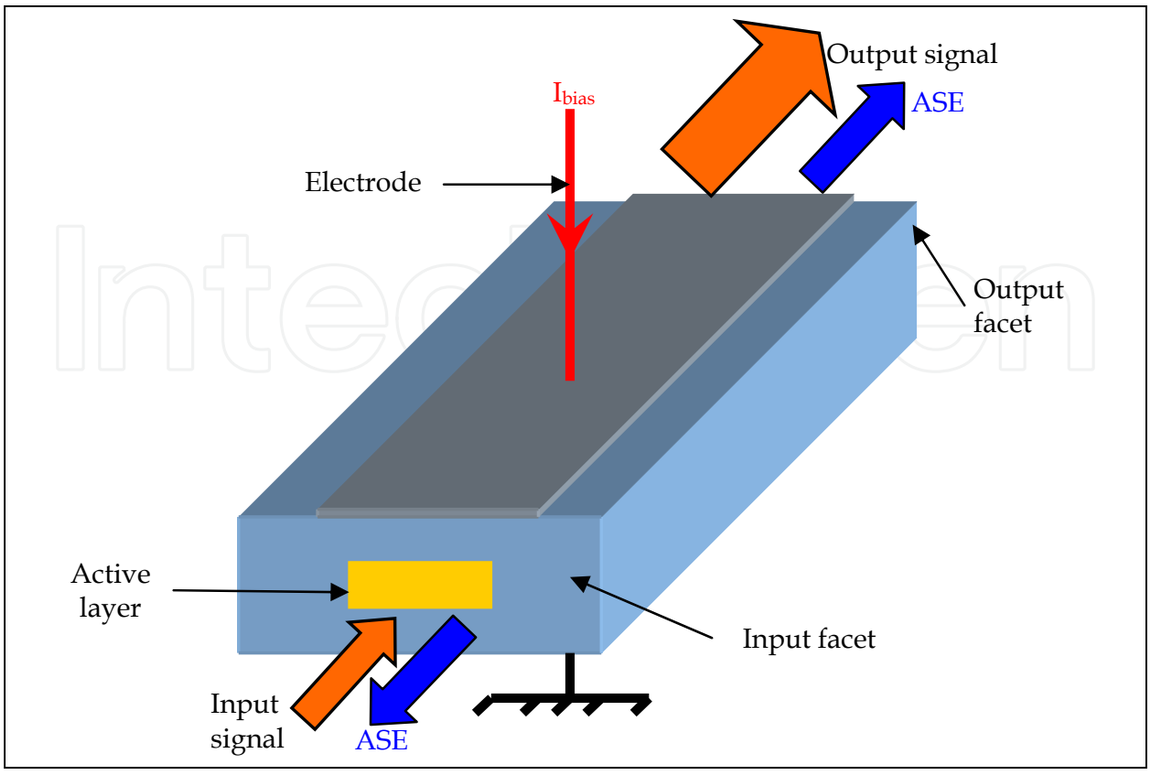

Fig. 1. SOA architecture.

Typical physical features of the SOA structure, used in simulations, are listed in Table 1.

Symbol	Description	Value
I_{bias}	Injection current	200 mA
η_{in}	Input coupling loss	3 dB
η_{out}	Output coupling loss	3 dB
R_1	Input facet reflectivity	5e-005
R_2	Output facet reflectivity	5e-005
L	Active layer length	500 μm
W	Active layer width	2.5 μm
d	Active layer height	0.2 μm
Γ	Optical confinement factor	30%
v_g	Group velocity	75 000 000 m/s
n_r	Active refractive index	3.7

Table 1. SOA parameters used in simulation.

2.2 SOA structure characteristics

The SOA has proven to be a versatile and multifunctional device that will be a key building block for next generation of optical networks. The parameters of importance, used to characterize SOAs, are:

- the gain bandwidth,

- the gain saturation,
- the noise figure,
- the polarisation independence,
- the conversion efficiencies,
- the input dynamic range,
- the extinction ratio/crosstalk,
- the tuning speed,
- the wavelength of operation.

The evolution of the SOA output power as function of the wavelength for various values of the input power is represented in figure 2. It shows that when the wavelength increases, the output power decreases. So, we can notice that when the input power injected into the SOA increases, the maximum of the output power will be moved towards the high wavelengths, which is due to the decrease of the carriers' density. For example, for an input power of - 18 dBm, the maximal output power is 5,41 dBm for a wavelength equal to 1520 nm; but for an injected power equal to -5 dBm, the maximum of the output power is 8,29 dBm and corresponds to a wavelength of 1540 nm. Whereas for an input power equal to 5 dBm, the maximal value of the output power is 8,95 dBm for a wavelength of 1550 nm.

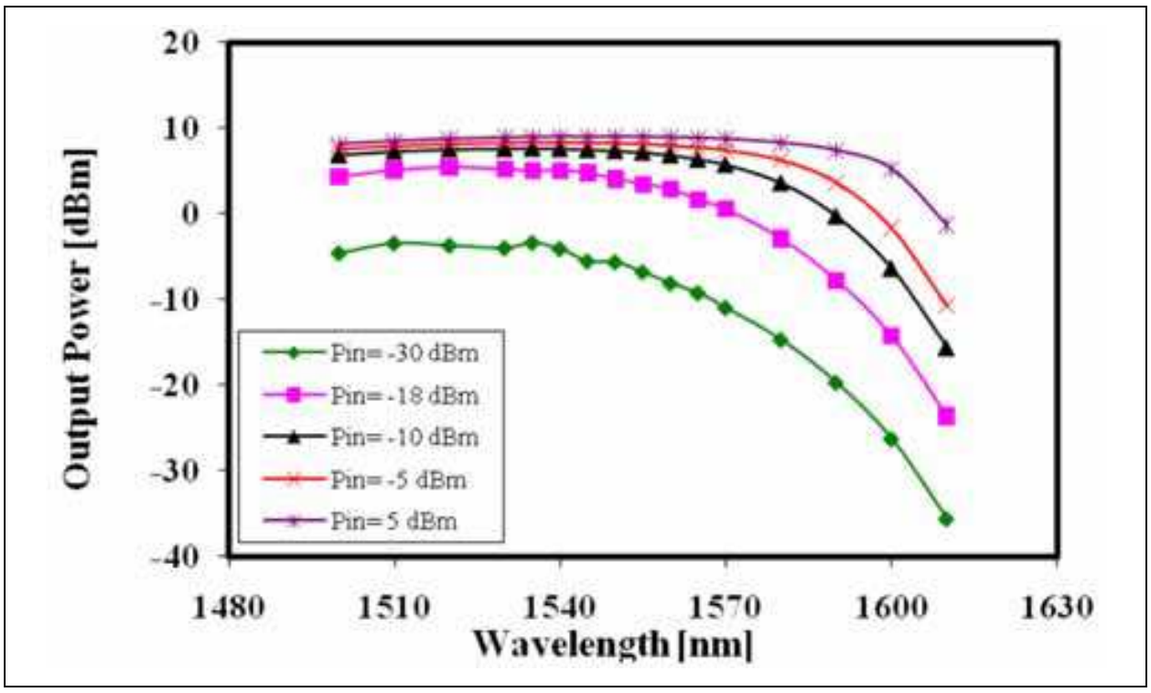

Fig. 2. SOA output power versus the wavelength of operation for different input powers.

A wide optical bandwidth is a desirable feature for a SOA, so that it can amplify a wide range of signal wavelengths. In order to analyze the impact of the injection condition on this parameter, we represent simulation results of the SOA gain as function of the wavelength of the signal for different input powers. Referring to figure 3, we note that wavelength variations and the injected power have a significant impact on the gain bandwidth evolution. However, we can notice according to the obtained curves, which are drawn for a bias current of 200 mA, that when the input power increases, the gain maximum (known as the peak of the gain) is

moved towards the high wavelengths, which is due to the decrease of the carriers' density. For an input power of -30 dBm, the gain peak is 26,6 dB at a wavelength equal to 1510 nm, but for an injected power of -10 dBm, the gain maximum is 17,65 dBm for a wavelength of 1535 nm. On the other hand, for a high input power of 5 dBm, for example, the gain peak, having a value of 3,96 dB, is reached for a signal wavelength of 1550 nm, which is higher than the wavelength corresponding to the last case.

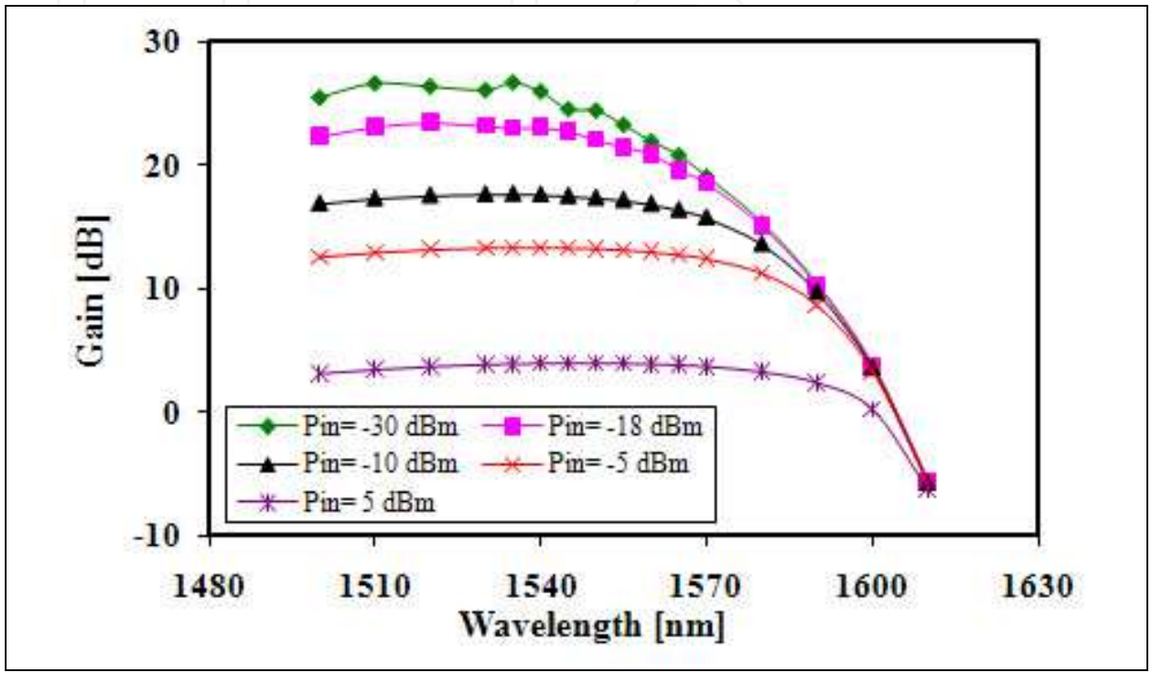

Fig. 3. Gain spectrum as a function of the injected input power.

In order to look for the conditions which correspond to an improvement of the SOA functioning, we have analyzed the influence of the intrinsic parameters on the SOA performance by representing, in figure 4, the gain and the noise figure as function of the bimolecular recombination coefficient (B). We notice that the increase of the B coefficient entails a diminution of the gain and consequently an increase of the noise figure. These results are justified by the fact that when the B coefficient increases, there will be an increase of the carriers' losses that are caused by the radiative and non-radiative recombination processes and consequently the carriers' density decreases, which involves a gain decrease. In that case, the maximal value of the gain is 26,16 dB, which corresponds to a minimum of noise figure of 5,27 dB, a B coefficient equal to 9.10^{-16} $m^3.s^{-1}$ and an input power P_{in}= -30 dBm.

2.3 Noise effects in a SOA structure

One of major processes to consider in the SOA analysis is the amplified spontaneous emission (ASE) noise, because it strongly affects the structure performance. It is also crucial in determining the bit error rate (BER) of the transmission system within which the amplifier resides. The injected signal and the ASE noise interact nonlinearly as they propagate along the SOA structure. Then, the interaction correlates different spectral components of the noise. Consequently, we can distinguish three types of noise, which are:

- The shot noise.
- The signal-spontaneous beat noise.
- The spontaneous-spontaneous beat noise.

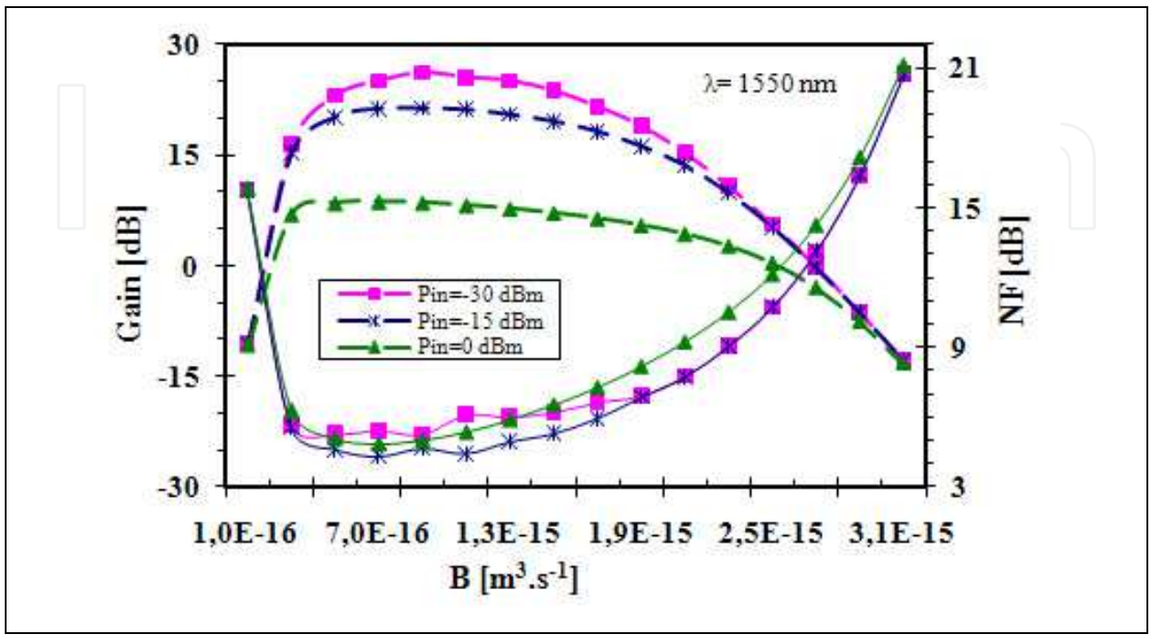

Fig. 4. Evolution of the gain and the noise as a function of the bimolecular recombination coefficient (B) and the SOA injected power.

The power of the ASE noise generated internally within the SOA is given by:

$$P_{ASE} = 2.n_{sp}.h.\nu.(G-1).B_0 \tag{1}$$

Where:
G: is the gain at the optical frequency ν,
h: represents the Planck's constant,
B_0: is the optical bandwidth of a filter within which P_{ASE} is determined,
n_{sp}: refers to the population inversion factor (sometimes called the spontaneous emission factor).
For an ideal amplifier, n_{sp} is equal to 1, corresponding to a complete inversion of the medium. However, in the usual case, the population inversion is partial and so $n_{sp} > 1$.
The shot noise results in the detection of the received total optical power due to the signal and the power of the ASE noise. It is given by the following equation:

$$N_{shot} = 2.e^2.B_e\left(\frac{G.P_{in}}{h.\nu} + n_{sp}.B_0.(G-1)\right) \tag{2}$$

Where B_e is the electrical bandwidth of the photo-detector.
The noise contribution due to the signal exists as well there is no optical amplifier; this later simply modifies the signal power, then the shot noise power related to this introduces a supplementary shot noise that is associated to the detection of the ASE.

The two intrinsic components related to beat noise are produced when optical signals and ASE coexist together. The first type of beat noise which is the signal-spontaneous beat noise occurs between optical signals and ASE having frequency close to that of the optical signals. It is given by the following equation:

$$N_{s-sp} = 4.\frac{e^2}{h.\nu}.B_e.P_{in}.n_{sp}.G.(G-1) \tag{3}$$

The second type, which is the spontaneous-spontaneous beat noise, occurs between ASEs. It is expressed as follows:

$$N_{sp-sp} = e^2.(2B_0 - B_e).B_e.n_{sp}^2.(G-1)^2 \tag{4}$$

The signal-spontaneous beat noise is preponderant for a strong input signal, whereas the spontaneous-spontaneous beat noise is dominating when there is an injection of a small input power. Compared to the shot noise and the signal-spontaneous beat noise, the spontaneous-spontaneous beat noise can be significantly minimized by placing an optical filter having a bandwidth B_0 after the amplifier.

A convenient way to quantify and characterize the noise and describe its influence on the SOA performance is in terms of Noise Figure (NF) parameter. It represents the amount of degradation in the signal to noise ratio caused by amplification process, and it is defined as the ratio between the optical signal to noise ratio (OSNR) of the signal at the input and output of SOA:

$$NF = \frac{OSNR_{in}}{OSNR_{out}} \tag{5}$$

The OSNR of the input signal is given by the following equation (Koga & Matsumoto, 1991):

$$OSNR_{in} = \frac{P_{in}}{2.h.\nu.B_e} \tag{6}$$

The OSNR of the input signal is proportional to the optical power of the input signal, or more specifically to the input number of photons per unit time ($P_{in}/h\nu$). Whereas, the OSNR of the output signal is defined by:

$$OSNR_{out} = \left(\frac{e.P_{in}.G}{h.\nu}\right)^2.\frac{1}{N_{shot} + N_{s-sp} + N_{sp-sp}} \tag{7}$$

Accordingly, by substituting equations (2), (3), (4), (6) and (7) into (5), the noise figure can be written as follows:

$$NF = \frac{1}{G} + 2.n_{sp}.\frac{G-1}{G} + \frac{h.\nu.B_0.n_{sp}.P_{in}.(G-1)}{P_{out}^2} + \frac{h.\nu.(2B_0 - B_e).n_{sp}^2.P_{in}.(G-1)^2}{2.P_{out}^2} \tag{8}$$

In practical case, the last two terms can be neglected because the ASE power is weak compared with the signal power; otherwise the spontaneous-spontaneous beat noise can be

minimized by placing an optical filter at the output. So the noise figure can be rewritten as (Simon et al., 1989):

$$NF \approx \frac{1}{G} + 2.n_{sp}.\frac{G-1}{G} \tag{9}$$

Since spontaneous emission factor (n_{sp}) is always greater than 1, the minimum value of NF is obtained for n_{sp}=1. So, for large value of gain (G>>1), the noise figure of an ideal optical amplifier is 3dB. This is considered as the lowest NF that can be achieved. This implies that every time an optical signal is amplified, the signal to noise ratio is reduced to the half.
The NF can be expressed as function of the power of ASE noise, which is given by (1), as follows:

$$NF \approx \frac{1}{G} + 2.\frac{P_{ASE}}{h.\nu.G.B_0} \tag{10}$$

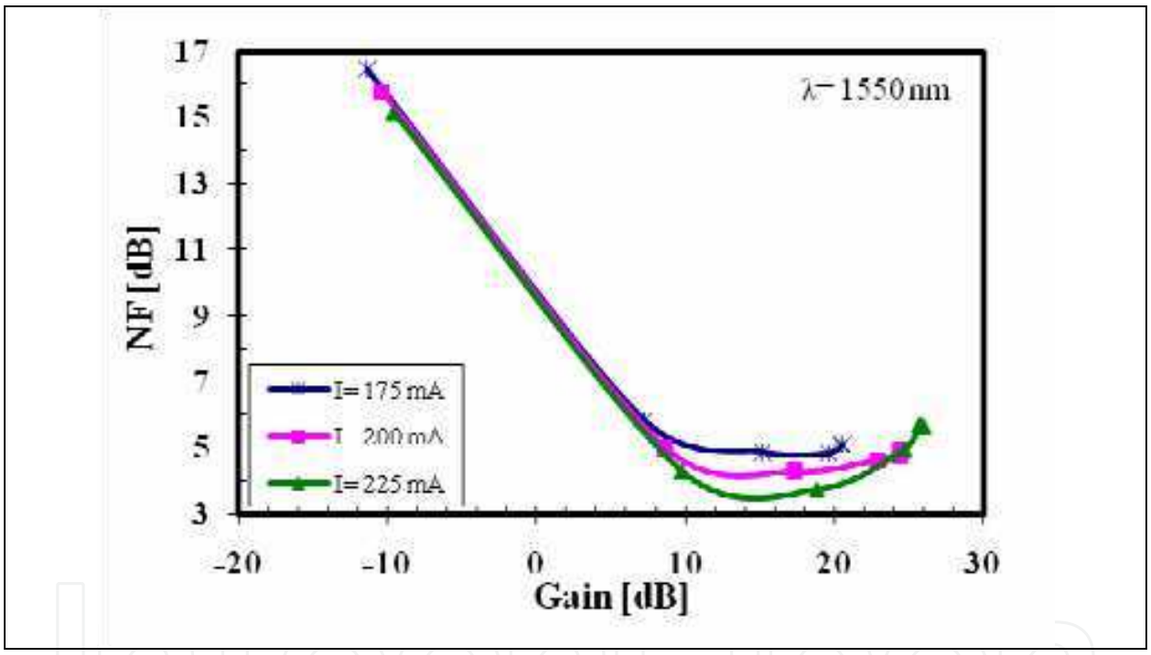

Fig. 5. Evolution of the noise figure as a function of the SOA gain for different bias current values.

The NF is represented as function of the gain in figure 5. This result is very significant because it allows us to choose the characteristics of the SOA in order to obtain the highest value of the gain for a minimum noise figure. So, we can notice that a low gain corresponds to a high value of NF; whereas to have the possible maximum of the gain while satisfying the criterion of low noise, it is necessary to choose the highest bias current possible.

2.4 Linear and saturation operating regimes in a SOA structure

A SOA amplifies input light through stimulated emission by electrically pumping the amplifier to achieve population inversion. It should have large enough gain for such application. The gain is dependent on different parameters, such as the injected current, the

device length, the wavelength and the input power levels. The SOA gain decreases as the input power is increased.
This gain saturation of the SOA is caused not only by the depletion of carrier density owing to stimulated emission, but also by the main intraband processes, such as spectral hole burning (SHB) and carrier heating (CH). However, when the SOA is operated with pulses shorter than a few picoseconds, intraband effects become important.
The origin of gain saturation lies in the power dependence of the gain coefficient where the population inversion due to injection current pumping is reduced with the stimulated emission induced by the input signal.
The saturation power parameter of the SOAs is of practical interest. It is a key parameter of the amplifier, which influences both the linear and non-linear properties. It is defined as the optical power at which the gain drops by 3 dB from the small signal value. That is to say, it is the optical power which reduces the modal gain to half of the unsaturated gain.
The saturation output power of the SOA is given by (Connelly, 2002):

$$P_{sat} = \frac{A}{\Gamma}.I_s \tag{11}$$

Where:

$$I_s = \frac{h.\nu}{a_N.\tau_s} \tag{12}$$

A: denotes the active region cross-section area,
Γ: represents the optical confinement factor coefficient,
a_N: symbolizes the differential modal gain,
τ_s: makes reference to spontaneous carrier lifetime.
High saturation output power is a desirable SOA characteristic, particularly for power booster and multi-channel applications. Referring to equation (11), the saturation output power can be improved by increasing the saturation output intensity (I_s) or reducing the optical confinement factor. The former case can be achieved either by reducing the differential modal gain and/or the spontaneous carrier lifetime. Since the last parameter (τ_s) is inversely proportional to carrier density, operation at a high bias current leads to an increase in the saturation output power. Nevertheless, when the carrier density increases, the amplifier gain also increases, making resonance effects more significant.
As the saturation output power depends inversely on the optical confinement factor, the single pass gain can be maintained by reducing this coefficient or by increasing the amplifier length. This process is not always necessary for the reason that the peak material gain coefficient shifts to shorter wavelengths as the carrier density is increasing.
When the average output power is at least 6 dB less than the output saturation power, non-linear effects are not observed and the SOA is in the linear regime. This linear operating regime, which is closely related to the output saturation power, is defined as the output power of an SOA where the non-linear effects do not affect the input multi-channel signal.
Gain saturation effects introduce undesirable distortion to the output signal. So, an ideal SOA should have very high saturation output power to achieve good linearity and to maximize its dynamic range with minimum distortion. Moreover, high saturation output power is desired for using SOAs especially in wavelength division multiplexing (WDM)

systems. Figure 6 shows that the highest value of the saturation output power, which corresponds to very fast dynamics of the carriers' density, is obtained when a strong bias current is used. Furthermore, we can notice that a high value of the bias current can engender a high gain with a high saturation output power. On the other hand, a low bias current corresponds to a less strong gain with a less high saturation output power, but the saturation input power is stronger.

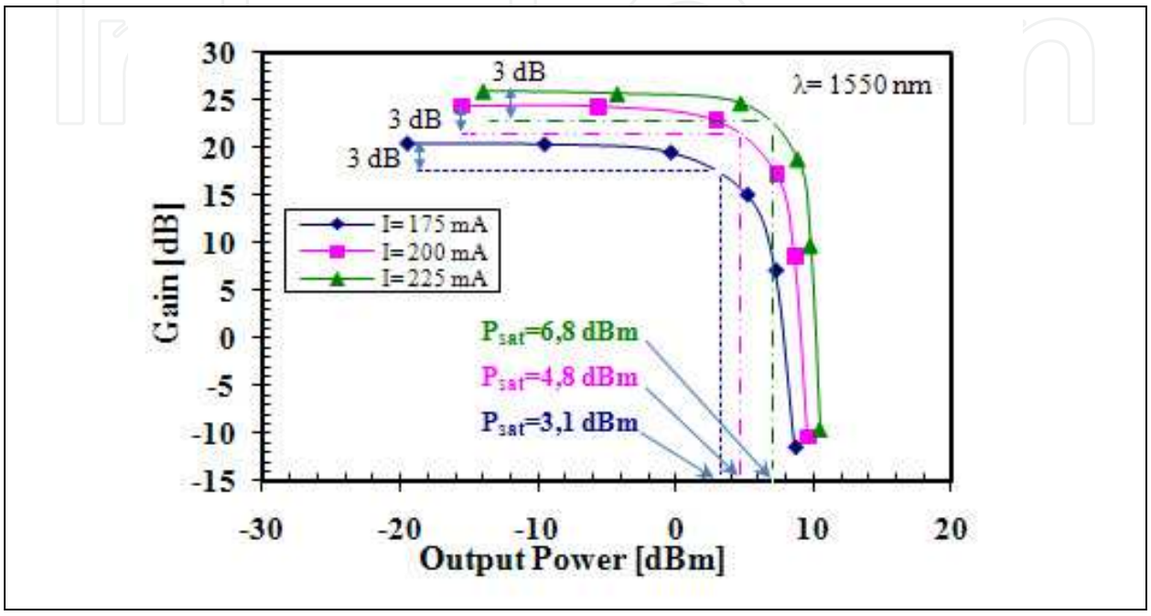

Fig. 6. Evolution of the gain as a function of the output power and the SOA bias current.

Because of the SOA's amplification and nonlinear characteristics, SOAs or integrated SOAs with other optical components can be exploited to assure various applications for high bit rate network systems. Moreover, large switching matrices comprised of SOA gates can be constructed to take advantage of the SOA gain to reduce insertion losses, to overcome electronic bottlenecks in switching and routing. The fast response speed can also be utilized effectively to perform packet switching.

3. SOA nonlinearities

SOAs are showing great promise for use in evolving optical networks and they are becoming a key technology for the next generation optical networks. They have been exploited in many functional applications, including switching (Kawaguchi, 2005), wavelength conversion (Liu et al., 2007), power equalization (Gopalakrishnapillai et al., 2005), 3R regeneration (Bramerie et al., 2004), logic operations (Berrettini et al., 2006), etc., thanks to their nonlinear effects, which are the subject of the current section. The effects are: the self gain modulation (SGM), the self phase modulation (SPM), the self induced nonlinear polarization modulation (SPR), the cross-gain modulation (XGM), the cross-phase modulation (XPM), the four-wave mixing (FWM) and the cross-polarization modulation (XPolM). These functions, where there is no conversion of optical signal to an electrical one, are very useful in transparent optical networks.

In SOA operational regime, there is a variation of the total density of the carriers and their distributions. This variation engenders intraband and interband transitions. The interband transition changes the carrier density but does not affect the carrier distribution. It is produced by the stimulated emission, the spontaneous emission and the non-radiative recombination. The modification of the total density of the carriers comes along with the modification of the carriers in the same band. The intraband transitions, such as spectral hole burning (SHB) and carrier heating (CH) are at the origin of the fast dynamics of the SOAs. They change the carrier distribution in the conduction band.
The main nonlinear effects involved in the SOAs, having for origin carriers dynamics and caused mainly by the change of the carriers density induced by input signals, are the following ones:

3.1 Self Gain Modulation

The self gain modulation (SGM) is an effect which corresponds to the modulation of the gain induced by the variation of the input signal power. It can be used to conceive a compensator of signal distortion.

3.2 Self Phase Modulation

The self phase modulation (SPM) is a nonlinear effect that implies the phase modulation of the SOA output signal caused by the refractive index variation induced by the variation of the input signal power.

3.3 Self induced nonlinear Polarization Rotation

The self induced nonlinear polarization rotation (SPR) translates the self rotation of the polarization state of the SOA output signal with regard to input one.

3.4 Cross-Gain Modulation

The cross-gain modulation (XGM) is a nonlinear effect, which is similar to the SGM. It implies the modulation of the gain induced by an optical signal (known as a control or pump signal), which affects the gain of a probe signal propagating simultaneously in the SOA. The XGM can take place in a SOA with a co-propagative or counter-propagative configuration.

3.5 Cross-Phase Modulation

The cross-phase modulation (XPM) is a nonlinear effect, which is similar to the SPM. It corresponds to the change of the refractive index induced by an optical signal (known as a control or pump signal), which affects the phase of another optical signal (probe) propagating at the same time in the SOA structure.

3.6 Four Wave Mixing

The four wave mixing (FWM) is a parametric process, which is at the origin of the production of new frequencies. It can be explained by the beating between two or several optical signals having different wavelengths propagating in the SOA structure, which generates signals having new optical frequencies.
The FWM effect in SOAs has been shown to be a promising method for wavelength conversion. It is attractive since it is independent of modulation format, capable of

dispersion compensation and ultra fast. So, wavelength conversion based on FWM effect offers strict transparency, including modulation-format and bit-rate transparency, and it is capable of multi-wavelength conversions. However, it has low conversion efficiency and needs careful control of the polarization of the input lights (Politi et al., 2006). The main drawbacks of wavelength conversion based on FWM are polarization sensitivity and the frequency-shift dependent conversion efficiency.

3.7 Cross-Polarization Modulation

The cross-polarization modulation (XPolM) effect in a SOA structure, which has been subject of many investigations in recent years, is a nonlinear effect similar to the SPR. It denotes the polarization rotation of a beam propagating in a SOA affected by the polarization and the power of a relatively strong control beam, introduced simultaneously into the amplifier. When two signals are injected in the SOA, an additional birefringence and gain compression affects the SOA. The two signals affect one another by producing different phase and gain compression on the transverse electric (TE) and transverse magnetic (TM) components (because the gain saturation of the TE and TM modes is different). This results in a rotation of the polarization state for each signal. The SOA bias current, and the input signal power are among the parameters that determine the magnitude of the polarization rotation. As a result, the XPolM effect in SOA is then directly related to the TE/TM mode discrepancy of XPM and XGM.

The nonlinear polarization rotation that occurs in the SOA is demonstrated to perform very interesting functionalities in optical networks. However, it is exploited in optical gating, in wavelength conversion, in regeneration and in all-optical switching configurations that are required for wavelength routing in high-speed optical time-division multiplexing networks.

4. Modelling of polarization rotation in SOAs using the Coupled Mode Theory

4.1 Analysis of the polarization rotation in SOA with application of Stokes parameters

A convenient method to describe the state of polarization is in terms of Stokes parameters. They provide a very useful description of the polarization state of an electromagnetic wave. Moreover, they characterize the time-averaged electric-field intensity and the distribution of polarization among three orthogonal polarization directions on the Poincaré sphere. They are used in this work to analyze the polarization change at the SOA output with relation to its state at the input for various length of the active region. They are noted as (S_0, S_1, S_2, S_3) and defined as (Flossmann et al., 2006):

$$\begin{pmatrix} S_0 \\ S_1 \\ S_2 \\ S_3 \end{pmatrix} = \begin{pmatrix} A_{TE}{}^2 + A_{TM}{}^2 \\ A_{TE}{}^2 - A_{TM}{}^2 \\ 2A_{TE}.A_{TM}.\cos\left(\phi_{TM} - \phi_{TE}\right) \\ 2A_{TE}.A_{TM}.\sin\left(\phi_{TM} - \phi_{TE}\right) \end{pmatrix} \tag{13}$$

Where:

S_0 is a parameter that translates the total intensity.

S_1 refers to the intensity difference between the horizontal polarization and the vertical polarization.

S_2 makes reference to the difference between intensities transmitted by the axes (45°, 135°).

S_3 is a parameter that expresses the difference between intensities transmitted for the left and right circular polarizations.
ϕ_{TE} and ϕ_{TM} denote the phase shift for the TE and TM modes, respectively.
The normalized Stokes parameters that can be measured at the SOA structure output by using a polarization analyzer are given by:

$$s_i = \frac{S_i}{S_0} \quad \text{with i} \in \{1, 2, 3\} \tag{14}$$

The phase shift variation can be written as follows:

$$\Delta\phi = \phi_{TM} - \phi_{TE} = \arctan\left(\frac{s_3}{s_2}\right) \tag{15}$$

The relationship of the normalized Stokes parameters to the orientation (azimuth) and the ellipticity angles, ψ and χ, associated with the Poincaré Sphere is shown in the following equations (Guo & Connelly, 2005):

$$\begin{pmatrix} s_1 \\ s_2 \\ s_3 \end{pmatrix} = \begin{pmatrix} \cos(2\psi).\cos(2\chi) \\ \sin(2\psi).\cos(2\chi) \\ \sin(2\chi) \end{pmatrix} \tag{16}$$

Therefore, the polarization change at the SOA output can be analyzed and evaluated by the azimuth and the ellipticity that can be expressed as function of normalized Stokes parameters:

$$\begin{cases} \psi = \frac{1}{2}\arctan\left(\frac{s_2}{s_1}\right) \\ \chi = \frac{1}{2}\arcsin\left(s_3\right) \end{cases} \tag{17}$$

4.2 Concept of the proposed model

In this model, which is based on the coupled mode theory (CMT), we assume that the optical field is propagating in the z-direction of the SOA structure and it is decomposed into TE and TM component. In addition, the TE/TM gain coefficients are supposed, in a saturated SOA, to be not constant along the amplifier length and then can be written as the following forms (Connelly, 2002):

$$\begin{cases} g_{TE}(z) = \Gamma_{TE}.g_m(z) - \alpha_{TE} \\ g_{TM}(z) = \Gamma_{TM}.g_m(z) - \alpha_{TM} \end{cases} \tag{18}$$

Where g_{TE} and g_{TM} are the gain coefficients, Γ_{TE} and Γ_{TM} denote the confinement factors, α_{TE} and α_{TM} symbolize the efficient losses, respectively for TE and TM modes. g_m designates the gain material coefficient.
To estimate the polarization sensitivity of a saturated amplifier, the material intensity gain coefficient is assumed to be saturated by the light intensity as the following equation (Gustavsson, 1993):

$$g_m(z) = \frac{g_{m,0}}{1 + \left(\left|A_{TE}(z)\right|^2 + \left|A_{TM}(z)\right|^2 \right).E_s^{-2}} \tag{19}$$

Referring to the coupled mode equations developed in (Gustavsson, 1993) that take into account the coupling between the TE and TM modes, the evolution of the electromagnetic field envelope in the SOA active region can be written under the following equations:

$$\begin{cases} \dfrac{\partial A_{TE}}{\partial z} = \dfrac{1}{2} g_{TE}(z).A_{TE}(z) + C_{cpl,1}.A_{TM}(z).e^{-j.\Delta\beta.z} \\ \dfrac{\partial A_{TM}}{\partial z} = \dfrac{1}{2} g_{TM}(z).A_{TM}(z) - C_{cpl,2}.A_{TE}(z).e^{j.\Delta\beta.z} \end{cases} \tag{20}$$

Where

$\Delta\beta$ represents the difference between the propagation constants β_{TE} and β_{TM} for TE and TM modes, respectively.

$C_{cpl,i}$ (with i={1,2}) denotes the coupling coefficient given by the following equation:

$$C_{cpl,i}(z) = \kappa_i - \kappa_i.\left(1 + \frac{\left(\left|A_{TE}(z)\right|^2 + \left|A_{TM}(z)\right|^2 \right)}{\left|E_s\right|^2} \right)^{-1} - \kappa_i.\left(1 + \frac{\left(\left|A_{TE}(z)\right|^2 + \left|A_{TM}(z)\right|^2 \right)}{\left|E_s\right|^2} \right)^{-2} \tag{21}$$

With: "κ_i" is a constant.

Hence, the evolution of the electromagnetic field envelope in the active region of the SOA can also be written under the following matrix form:

$$\frac{\partial}{\partial z}\begin{pmatrix} A_{TE}(z) \\ A_{TM}(z) \end{pmatrix} = j.\begin{pmatrix} m_{11} & m_{12} \\ m_{21} & m_{22} \end{pmatrix}.\begin{pmatrix} A_{TE}(z) \\ A_{TM}(z) \end{pmatrix} \tag{22}$$

Where

$$\begin{cases} m_{11} = -\dfrac{j}{2}.(\Gamma_{TE}.g_m(z) - \alpha_{TE}) \\ m_{12} = -j.C_{cpl1}.e^{-j.\Delta\beta.z} \\ m_{21} = j.C_{cpl2}.e^{j.\Delta\beta.z} \\ m_{22} = -\dfrac{j}{2}.(\Gamma_{TM}.g_m(z) - \alpha_{TM}) \end{cases} \tag{23}$$

The solution of the set of differential equations (20) is not available in analytical form. Then, for calculating the electromagnetic field envelope in the SOA structure, it is primordial to use a numerical method; that is the object of the next section.

4.3 Numerical method formulation

The numerical method adopted to calculate electromagnetic field envelope of SOA, is based on a numerical integration approach of the differential equations in the z-direction. Firstly, the equation (22) is reformulated as:

$$\frac{\partial A(z)}{\partial z} = j.M\left(A(z)\right).A(z) \tag{24}$$

Where

$$A(z) = \begin{pmatrix} A_{TE}(z) \\ A_{TM}(z) \end{pmatrix} \tag{25}$$

$$M\left(A(z)\right) = \begin{pmatrix} m_{11} & m_{12} \\ m_{21} & m_{22} \end{pmatrix} \tag{26}$$

The initial solution of equation (24) at a position $z=z_0+\Delta z$ is given by:

$$A_0(z_0 + \Delta z) = A(z_0).\exp\left(-j.M(z_0).\Delta z\right) \tag{27}$$

For the fact that the matrix M is not constant in the interval Δz, it is necessary to apply a correction to the initial solution. The correction term is expressed as:

$$A_c(z_0 + \Delta z) = \frac{j.\Delta z}{2}\left[M(z_0 + \Delta z) - M(z_0)\right].\overline{A_0} \tag{28}$$

Where $\overline{A_0}$ is the average value of A(z) in the interval $[z_0, z_0+\Delta z]$.
Then, the final solution will be written as the following form:

$$A(z_0 + \Delta z) = A_0(z_0 + \Delta z) + A_c(z_0 + \Delta z) \tag{29}$$

For the numerical implementation of the described method, the exponential term in equation (27) is developed as a finite summation of Taylor series terms as:

$$A_0(z_0 + \Delta z) = \sum_{p=0}^{q} \frac{1}{p!}.\left(-j.\Delta z.M(z_0)\right)^p.A(z_0) + O^{q+1}(\Delta z) \tag{30}$$

In which $O^{q+1}(\Delta z)$ denotes that the remaining error is order (q+1) in Δz.
Finally, in order to reduce the calculation time, it is worthwhile to calculate the electromagnetic field envelope of SOA recursively as the following form:

$$\frac{1}{p!}.\left[-j.\Delta z.M(A(z_0))\right]^p.A(z_0) = \frac{\Delta z}{p!}.\left[-j.M(A(z_0))\right] * \frac{\Delta z^{p-1}}{(p-1)!}.\left[-j.M(A(z_0))\right]^{p-1}.A(z_0) \tag{31}$$

4.4 Numerical simulation results and their experimental validation

In the implementation of the developed model, which is proposed in the section 4.3, using the theoretical background described above, the Taylor series is evaluated up to the twentieth order. In order to validate the results obtained by this approach, we have performed an experiment which was done in free-space. Its setup consists of a commercial InGaAsP/InP SOA structure, which is positioned so that their TE and TM axes correspond to the horizontal and vertical axes of the laboratory referential, respectively. The laboratory refers to the RESO lab in the National Engineering School of Brest, France. Light emitted from the SOA was collected and collimated with a microscope objective, then passed through a quarter-wave plate and a linear polarizer acting as an analyzer, before being recollected with a fibred collimator, connected to an optical spectrum analyzer with an optical band-pass filter, having a bandwidth of 0.07 nm in order to reject the amplified

spontaneous emission. The passing axis of the linear polarizer, when set vertically, coincided with the TM axis in the sample and defined a reference direction from which the orientation angle θ of the fast axis of the quarter-wave plate was estimated. This orientation could be modified, as the quarter-wave plate was mounted on a rotation stage whose movements were accurately determined by a computer-controlled step motor.

The presence of an injected optical signal affects the carrier density and includes strong modifications of the birefringence and dichroism experienced by the signal itself in the SOA active zone. Consequently, the input optical signal experiences a modification of its polarization state due to the intrinsic birefringence and residual differential gain of the active region. In the linear operating regime, the SOA output polarization remains nearly independent of the input power. However, within the saturation regime, a self-induced nonlinear rotation of polarization takes place and depends upon input power, because of carrier density variations which modify induced birefringence and residual differential gain. This causes fast variations of the state of polarization of the output signal, both in terms of azimuth and ellipticity parameters, which are analyzed in this section by varying the SOA injection conditions.

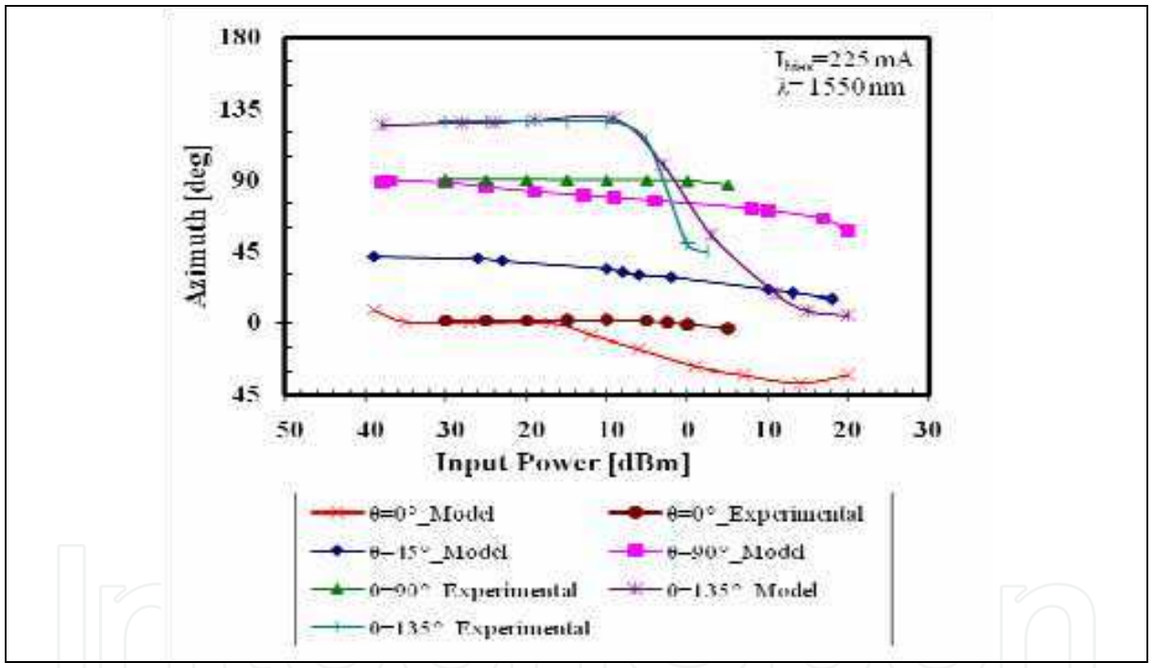

Fig. 7. Evolution of the azimuth of the output state of polarization of the SOA as a function of the injected input power for a bias current of 225 mA.

Figure 7 depicts the evolution of the azimuth at the output as a function of the input signal power initially injected at an angle θ. When θ = 0° or θ = 90°, the azimuth undergoes a small variation. Whereas, when θ = 45° or θ = 135° that corresponds to the injection with identical TE/TM powers, a significant change of the polarization state is shown when the input signal power becomes high, which corresponds to the saturation regime, contrarily for low values that refer to the linear operating regime. However, we can notice that the results obtained are in good agreement with the experimental measurements.

The ellipticity, which is shown in figure 8, experiences a slight increase when there is an augmentation of the injected power for an angle θ equal to 0° or 90°. However, for the case

of injecting the input power with θ = 45° or θ = 135°, the ellipticity parameter experiences significant variations.

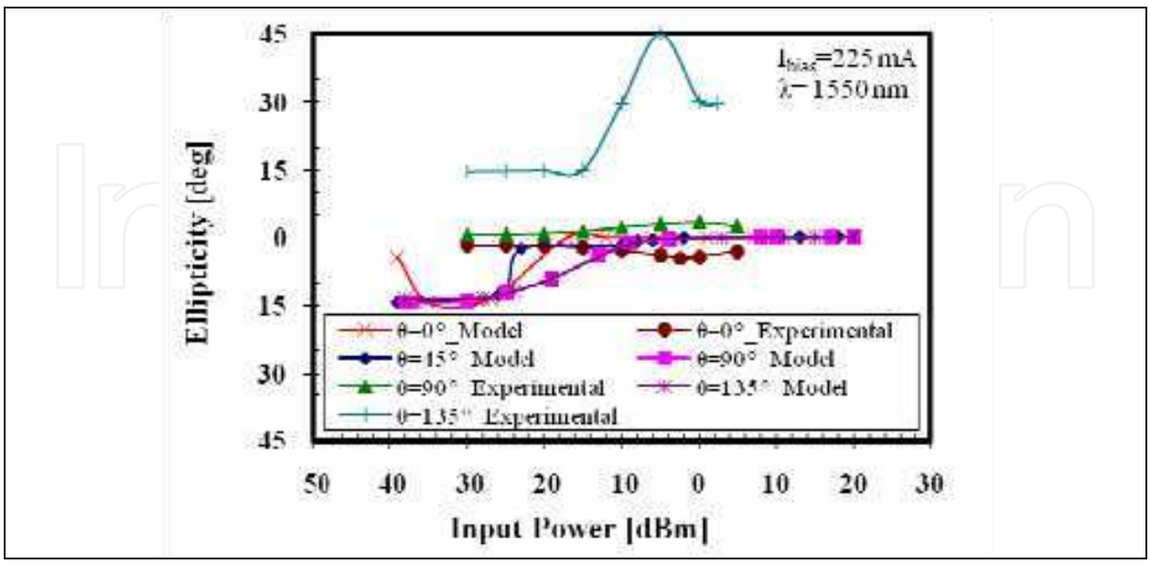

Fig. 8. Evolution of the ellipticity of the output state of polarization of the SOA versus the input signal power for a bias current of 225 mA.

According to the results presented in figure 9, we can notice that the phase shift is almost constant when the input signal power is very low. It decreases rapidly by augmenting the injected power. This behavior is explained by the diminution of carrier density due to the stimulated emission as the input power is increased. Also, it mirrors the variation of birefringence induced by effective refractive index variations with carrier densities. Moreover, this change of ΔΦ is significant only in the gain band; i.e. when the injected input power is high and thus corresponds to the operation at the saturation regime.

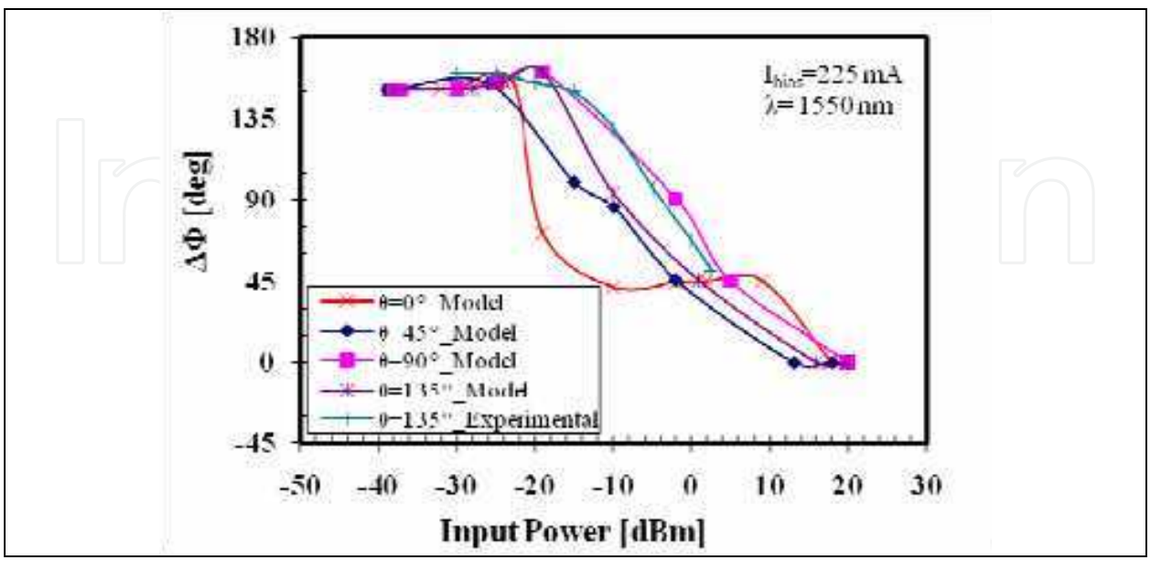

Fig. 9. Variation of the phase shift of the optical signal at the SOA output as a function of the injected input power for a bias current of 225 mA.

5. Application of SOA nonlinearities to achieve wavelength conversion

All-optical wavelength converters are considered key components in future WDM optical networks due to their main advantage that consists of increasing the flexibility and the capacity of these networks and facilitating WDM network management. Moreover, they form an essential part of the wavelength routing switch that is employed in the all-optical buffering concept. All-optical wavelength conversion can be realized by using fiber nonlinearities or nonlinearities in semiconductor devices.

In the last few years, a considerable attention has been focusing on SOAs and their potential use in optical communication systems. Especially, SOAs have generated more and more interest when optical signal processing is involved. Subsequently, they are exploited to achieve wavelength conversion at high bit rates, which is a very important function in conjunction with WDM systems. This reason makes them also very useful in wavelength routers, which manage wavelength paths through optical networks based on complex meshes, rather than point-to-point architectures (Wei et al., 2005).

Many studies have paid more attention on SOA performance for implementing and configuring wavelength conversion sub-systems. Hence, several optical wavelength converters based on SOA nonlinearities have been proposed and discussed, such as XGM (Tzanakaki & O'Mahony, 2000), XPM (Matsumoto et al., 2006), FWM (Contestabile et al., 2004), and XPolM (Wei et al., 2005). Each configuration has its advantages and disadvantages and thus its framework of application in optical communication networks.

Optical wavelength converters based on SOA nonlinearities, which are fundamental components in today's photonic networks, offer advantages in terms of integration potential, power consumption, and optical power efficiency. However, the major limitation of SOA-based wavelength converters is the slow SOA recovery, causing unwanted pattern effects in the converted signal and limiting the maximum operation speed of the wavelength converters. It has already been theoretically and experimentally clarified that the increase in electrical pumping power, confinement factor and the device interaction length effectively improve the speed performance (Joergensen et al., 1997). For improving the SOA-based wavelength converters, some techniques are proposed, such as: Fiber Bragg grating at 100 Gbit/s (Ellis et al., 1998), interferometric configuration at 168 Gbit/s (Nakamura et al., 2001), two cascaded SOAs at 170.4 Gbit/s (Manning et al., 2006) and optical filtering at 320 Gbit/s (Liu et al., 2007).

In this section, we evaluate the influence of SOA parameters and the signal format (non return-to-zero "NRZ" or return-to-zero "RZ") on the behavior of the structure used in wavelength conversion configuration and we analyze the performance dependence on several critical operation parameters of the SOA structure.

5.1 Concept of wavelength conversion based on SOA nonlinear effects

All-optical wavelength conversion refers to the operation that consists of the transfer of the information carried in one wavelength channel to another wavelength channel in the optical domain. It is a key requirement for optical networks because it has to be used to extend the degree of freedom to the wavelength domain. Moreover, All-optical wavelength conversion is also indispensable in future optical packet switching (OPS) networks to optimize the network performance metrics, such as packet loss rate and packet delay (Danielsen et al., 1998). Also, it is very useful in the implementation of switches in WDM networks. In addition, it is crucial to lower the access blocking probability and therefore to increase the utilization efficiency of the network resources in wavelength routed optical networks.

While a significant part of network design, routing and wavelength assignment depends on the availability and performance of wavelength converters; and as many techniques have been explored and discussed in this context, all-optical wavelength converters based on SOA structures have attracted a lot of interest thanks to their attractive features, such as the small size, the fast carrier dynamics, the multifunctional aspect and the high potential of integration. The main features of a wavelength converter include its transparency to bit rate and signal format, operation at moderate optical power levels, low electrical power consumption, small frequency chirp, cascadability of multiple stages of converters, and signal reshaping.

When a RZ pump (the data signal) at wavelength λ_1 and a continuous wave (CW) probe signal at wavelength λ_2 are injected into an SOA, the pump modulates the carrier density in its active region and hence its gain and refractive index. This leads to a change in the amplitude and phase of the CW probe signal. In the case of XGM, the output probe signal from the SOA carries the inverted modulation of the RZ input data signal.

The XPM is used to obtain an output probe signal with non-inverted modulation, whereby the phase modulation of the probe signal is converted to amplitude modulation by an interferometer. Particularly, in the wavelength conversion based on the XGM scheme, a strong input signal is needed to saturate the SOA gain and thereby to modulate the CW signal carrying the new wavelength. While the XGM effect is accompanied by large chirp and a low extinction ratio, and limited by the relatively slow carrier recovery time within the SOA structure, impressive wavelength conversion of up to 40 Gbit/s and with some degradation even up to 100 Gbit/s (Ellis et al., 1998), has been demonstrated.

To overcome the XGM disadvantages, SOAs have been integrated in interferometric configurations, where the intensity modulation of the input signal is transferred into a phase modulation of the CW signal and exploited for switching. These XPM schemes enable wavelength conversion with lower signal powers, reduced chirp, enhanced extinction ratios and ultra fast switching transients that are not limited by the carrier recovery time. Subsequently, wavelength conversion based on the XPM effect with excellent signal quality up to 100 Gbit/s, has been demonstrated (Leuthold et al., 2000) by using a fully integrated and packaged SOA delayed interference configuration that comprises a monolithically integrated delay loop, phase shifter and tunable coupler.

The FWM effect in SOAs has been shown to be a promising method for wavelength conversion. It is attractive since it is independent of modulation format, capable of dispersion compensation and ultra fast. So, wavelength conversion based on FWM offers strict transparency, including modulation-format and bit-rate transparency, and it is capable of multi-wavelength conversions. However, it has a low conversion efficiency and needs careful control of the polarization of the input lights (Politi et al., 2006). The main drawbacks of wavelength conversion based on FWM are polarization sensitivity and the frequency-shift dependent conversion efficiency.

Wavelength conversion based on XPolM is another promising approach. It uses the optically induced birefringence and dichroism in an SOA and it has great potential to offer wavelength conversion with a high extinction ratio.

The influence of the nonlinear polarization rotation and the intrinsic and extrinsic SOA parameters on the performance of a wavelength converter based on XGM effect is the subject of the next section.

5.2 Impact of polarization rotation on the performance of wavelength conversion based on XGM at 40 Gbit/s

Gain saturation of the SOA structure induces nonlinear polarization rotation that can be used to realize wavelength converters (Liu et al., 2003). Depending on the system configuration, inverted and non-inverted polarity output can be achieved. Recently, a remarkable wavelength conversion at 40 Gb/s with multi-casting functionality based on nonlinear polarization rotation has been demonstrated (Contestabile et al., 2005). The proposed wavelength converter based on XGM effect in a wideband traveling wave SOA (TW-SOA) at 40 Gbit/s, is presented in figure 10.

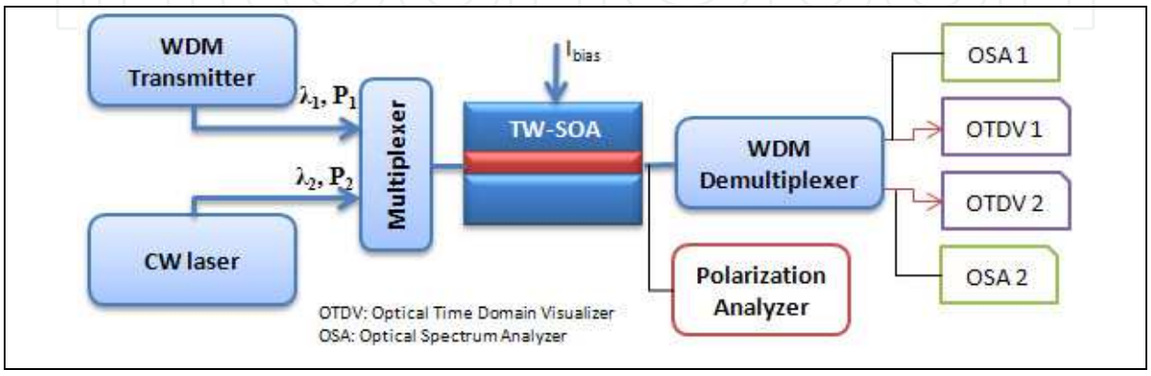

Fig. 10. Schematic of the wavelength converter configuration.

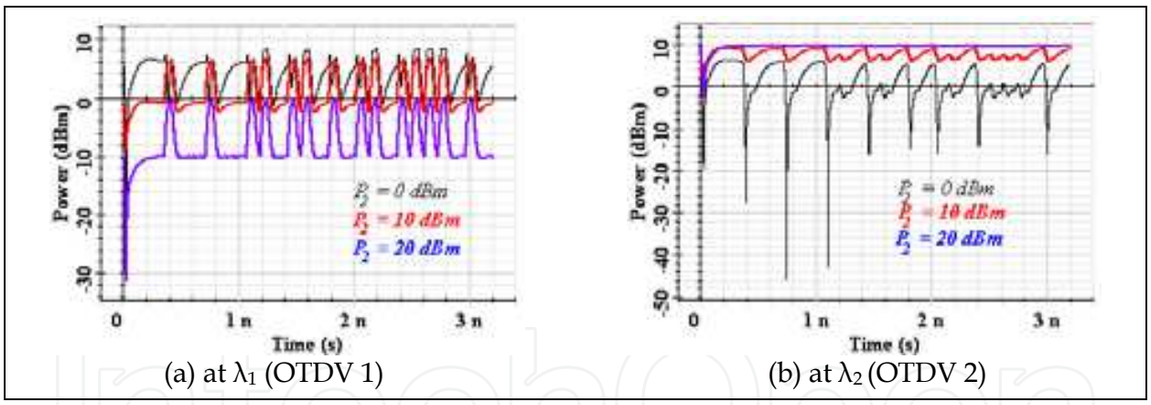

(a) at λ_1 (OTDV 1) (b) at λ_2 (OTDV 2)

Fig. 11. Evolution of the output signal by varying the CW input power for an RZ format signal.

An input signal obtained from a WDM transmitter, called the pump, at the wavelength λ_1= 1554 nm and a CW signal, called the probe light, at the desired output wavelength λ_2=1550 nm are multiplexed and launched co-directionally in the wideband TW-SOA. The pump wave modulates the carrier density and consequently the gain of the SOA. The modulated gain modulates the probe light, so that the output probe light, which is known as the converted signal, contains the information of the input signal, and achieve wavelength conversion (from λ_1 to λ_2).

By varying the CW input power and the input format signal, we visualized the output signal power by using the OTDV1 and OTDV2, as illustrated in figures 11 and 12. So, we can notice that a strong input signal is needed to saturate the SOA gain and thereby to

modulate the CW signal, as shown in figures 11b and 12b. Also, this is accompanied by a modulation inversion of the output signal, which is considered one among the drawbacks of the wavelength conversion using XGM.

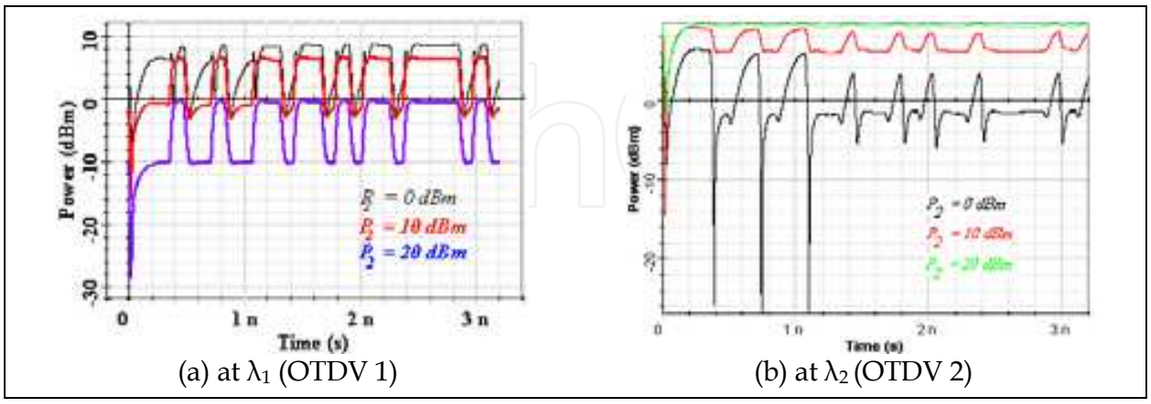

(a) at λ_1 (OTDV 1) (b) at λ_2 (OTDV 2)

Fig. 12. Evolution of the output signal power as a function of the CW power for an NRZ format signal.

Birefringent effects are induced when the pump is coupled into the structure, owing to the TE/TM asymmetry of the confinement factors, the carriers' distributions, the induced nonlinear refractive indices and the absorption coefficients of the SOA. Consequently, the linear input polarization is changed and becomes elliptical at the output as the input power is increased. Thus, the azimuth and ellipticity vary at the SOA output, as shown in figure 13a. A significant change of the polarization state is shown when the CW input power is high, contrarily for low values that correspond to a linear operating regime. Moreover, this polarization rotation varies not only with the pump power but also as a function of the RZ/NRZ signal format and the optical confinement factor.

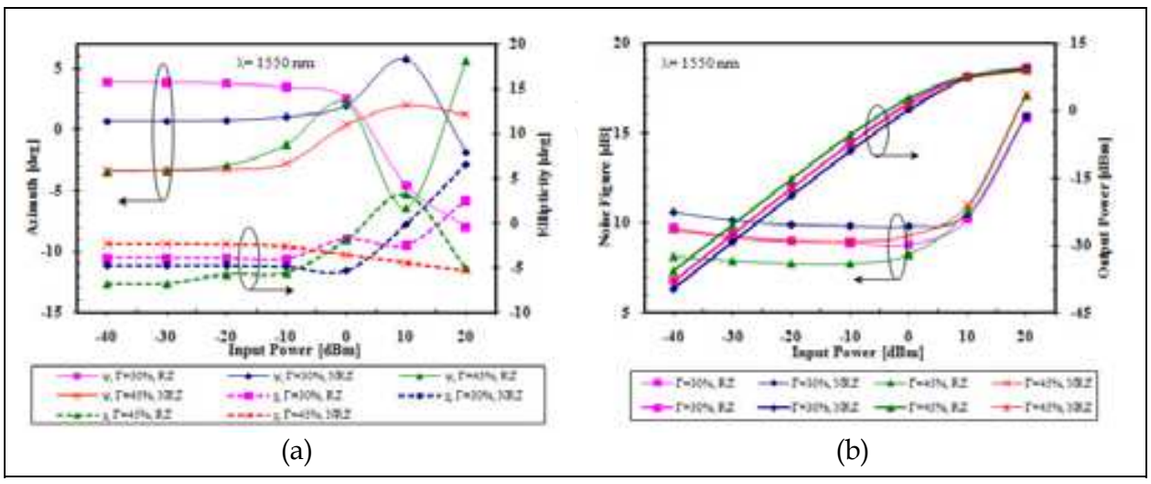

(a) (b)

Fig. 13. Evolution of the azimuth, the ellipticity, the noise figure and the output power as a function of the input signal power, the signal format and the optical confinement factor.

The transfer function, illustrated in figure 13b, shows that the linear operating regime is exhibited when the input power is low; then the RZ signal format with a high optical confinement factor is the privileged case. The saturation regime occurs as we are increasing the input powers, which corresponds to a gain saturation that can cause significant signal distortion at the output of the wavelength converter. Consequently, in the proposed wavelength converter scheme, we can use a band-pass filter just after the SOA, centered on λ_2 to suppress the spontaneous noise and to extract only the converted signal containing the information of the input signal. Moreover, the discussed wavelength converter configuration can be used to interface access-metro systems with the core network by achieving wavelength conversion of 1310 to 1550 nm since multi-Gbit/s 1310 nm transmission technology is commonly used in access and metro networks and the long-haul core network is centered on 1550 nm window.

In order to analyze the wavelength converter performance in detail, we adopt a wavelength conversion scheme based on an RZ configuration. The used SOA has a bias current I= 150mA and is connected to a receiver composed of a Bessel optical filter centered on λ_2, a photo-detector PIN, a low pass Bessel filter and a Bit-Error-Rate (BER) analyzer. The default order of the Bessel optical filter was set to 4 in the subsequent simulations.

By varying the input power, the maximum value for the Q-factor, the minimum value for the BER, the eye extinction ratio and the eye opening factor versus decision instant are shown in figures 14 and 15.

The results obtained demonstrate that the optimal point corresponds to an input power equal to -39 dBm. The BER analyzer eye diagram for this case is represented in figure 16. As for the order of the Bessel low pass filter at the receiver, it has been also studied to observe its effects on performance of the system. It appears from figure 16, that the change of the filter order "m" has a slight variation on the performance of the simulated system.

So, we can conclude that high-speed wavelength conversion seems to be one of the most important functionalities required to assure more flexibility in the next generation optical networks, since wavelength converters, which are the key elements in future WDM networks, can reduce wavelength blocking and offer data regeneration.

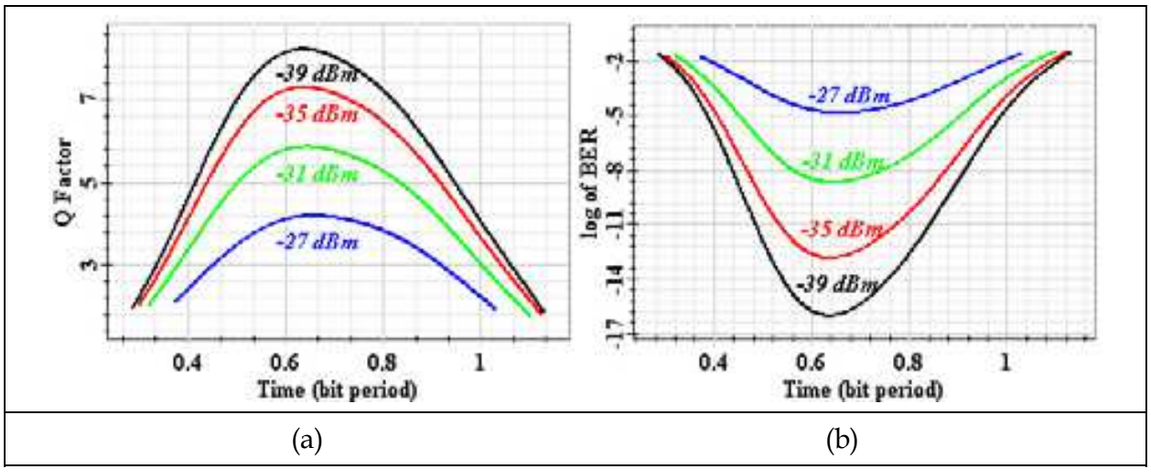

(a) (b)

Fig. 14. Evolution of the Q-factor and the BER for different values of the input power.

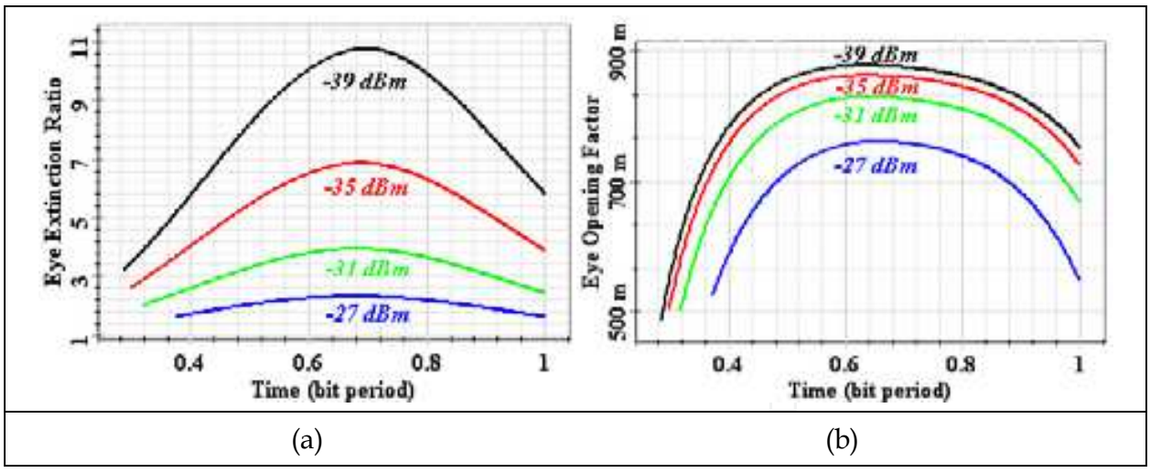

(a) (b)

Fig. 15. Evolution of the eye extinction ratio and the eye opening factor for different values of the input power.

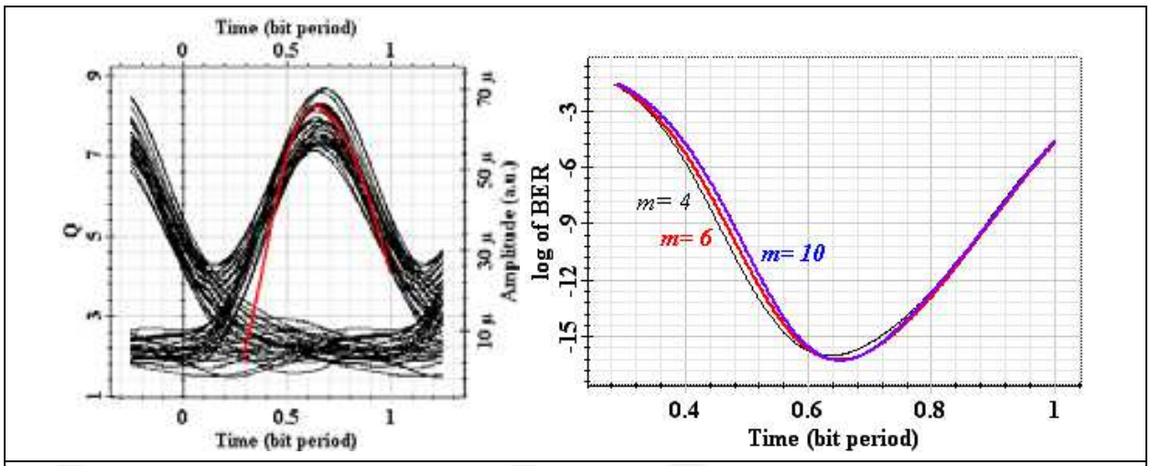

(a) (b)

Fig. 16. Evolution the eye diagram, the Q factor and the BER by changing the order of the Bessel low pass filter "m" for an input power equal to -39 dBm.

6. Conclusion

In this chapter, an investigation of SOA nonlinearities and their applications for future optical networks are presented and discussed. We have shown that intrinsic and extrinsic SOA parameters, such as the bias current, the active region length, etc. play an important role in the SOA gain dynamics. As results, high saturation output power, which is especially preferred in WDM systems, can be achieved by increasing the bias current or by using short SOAs. An accurate choice of these parameters is very important for the determination of the best device operation conditions to achieve the desired functionality based on SOAs and

exploiting their linear or saturation operating regime in a variety of different applications for all-optical signal processing and in long-haul optical transmissions.
We have also analyzed the impact of SOA parameter variations on the polarization rotation effect, which is investigated referring to a numerical model that we developed based on the Coupled Mode Theory and the formalism of Stokes. Subsequently, it is shown that the azimuth and the ellipticity parameters undergo changes according to injection conditions. Our model agrees well with available experimental measurements that have been carried out in free space and also reveals the conditions for the validity of previous simpler approaches.

7. References

Berrettini, G.; Simi, A.; Malacarne, A.; Bogoni, A. & Poti, L. (2006). Ultrafast integrable and reconfigurable XNOR, AND, NOR, and NOT photonic logic gate. *IEEE Photon. Technol. Lett.*, Vol. 18, No. 8, (Apr. 2006), (917-919), ISSN 1041-1135.

Bramerie, L.; Gay, M.; Girault, G.; Roncin, V.; Feve, S. & Simon, J.C. (2004). Performance of a Polarization Insensitive 3R Optical Regenerator Based on a new SOA-NOLM Architecture. *Proceedings of ECOC*, paper We2.5.2, Stockholm, 2004.

Connelly, M.J. (2002). *Semiconductor Optical Amplifier*, Kluwer Academic Publishers, ISBN 0-7923-7657-9, Boston, London.

Contestabile, G.; Presi, M. & Ciaramella, E. (2004). Multiple wavelength conversion for WDM multicasting by FWM in an SOA. *IEEE Photon. Technol. Lett.*, Vol. 16, No. 7, (Jul. 2004), (1775–1777), ISSN 1041-1135.

Contestabile, G.; Calabretta, N.; Presi, M. & Ciaramella, E. (2005). Single and multicast wavelength conversion at 40 Gb/s by means of fast nonlinear polarization switching in an SOA. *IEEE Photon. Technol. Lett.*, Vol. 17, No. 12, (Dec. 2005), (2652–2654), ISSN 1041-1135.

Danielsen, S.; Hansen, P. & Stubkjaer, K.E. (1998). Wavelength conversion in optical packet switching. *J Lightwave Technology*, Vol. 16, No. 12, (Dec. 1998), (2095–2108), ISSN 0733-8724.

Ellis, A.D.; Kelly, A.E.; Nesset, D; Pitcher, D.; Moodie, D.G. & Kashyap, R. (1998). Error free 100 Gb/s wavelength conversion using grating assisted cross gain modulation in 2 mm long semiconductor amplifier. *Electronics Lett.*, Vol. 34, No. 20, (Oct. 1998), (1958–1959), ISSN 0013-5194.

Flossmann, F.; Schwarz, U.T.; Maier, M. & Dennis, M.R. (2006). Stokes parameters in the unfolding of an optical vortex through a birefringent crystal. *J Optics Express*, Vol. 14, No. 23, (Nov. 2006), (11402-11411).

Gopalakrishnapillai, B.S.; Premaratne, M.; Nirmalathas, A. & Lim, C. (2005). Power Equalization using polarization rotation in semiconductor optical amplifiers. *IEEE Photon. Technol. Lett*,. Vol. 17, No. 8, (Aug. 2005), (1695-1697), ISSN 1041-1135.

Guo, L.Q. & Connelly, M.J. (2005). Signal-Induced Birefringence and Dichroism in a Tensile-Strained Bulk semiconductor optical amplifier and its Application to Wavelength Conversion. *J Lightwave Technology*, Vol. 23, No. 12, (Dec. 2005), (4037-4045), ISSN 0733-8724.

Gustavsson, M. (1993). Analysis of Polarization Independent Optical Amplifiers and Filters Based on Polarization Rotation in Periodically Asymmetric Waveguides. *IEEE J Quantum Electronics*, Vol. 29, No. 4, (Apr. 1993), (1168-1178), ISSN 0018-9197.

Joergensen, C.; Danielsen, S.L.; Stubkjaer, K.E.; Schilling. M.; Daub, K. & Doussiere, P. (1997). All-optical wavelength conversion at bit rates above 10 Gb/s using semiconductor optical amplifiers. *IEEE J Select. Top. Quantum Electron.*, Vol. 3, No. 5, (Oct. 1997), (1168–1180), ISSN 1077-260X.

Kawaguchi, H. (2005). All-Optical Switching of Picosecond Pulses by Four-Wave Mixing in a Semiconductor Optical Amplifier, In: *IPAP Books 2: Photonics Based on Wavelength Integration and Manipulation*, (271–282), Japan.

Koga, M. & Matsumoto, T. (1991). High-gain polarization-insensitive optical amplifier consisting of two serial semiconductor laser amplifiers. *J Lightwave Technology*, Vol. 9, No. 3, (Feb. 1991), (284–290), ISSN 0733-8724.

Leuthold, J.; Joyner, C.H.; Mikkelsen, B.; Raybon, G.; Pleumeekers, J.L.; Miller, B.I.; Dreyer, K. & Burrus, C.A. (2000). 100Gbit/s all-optical wavelength conversion with integrated SOA delayed-interference configuration. *Electronics Lett.*, Vol. 36, No. 13, (Jun 2000), (1129–1130), ISSN 0013- 5194.

Liu, Y.; Hill, M.T.; Tangdiongga, E.; de Waardt, H.; Galabretta, N. & Khoe, G.D. (2003). Wavelength conversion using nonlinear polarization rotation in a single semiconductor optical amplifier. *IEEE Photon. Technol. Lett,*. Vol. 15, (2003), (90–92), ISSN 1041-1135.

Liu, Y.; Tangdiongga, E.; Li, Z.; de Waardt, H.; Koonen, A.M.J.; Khoe, G.D.; Xuewen, S.; Bennion, I. & Dorren, H.J.S. (2007). Error-free 320-Gb/s all-optical wavelength conversion using a single semiconductor optical amplifier. *IEEE J Lightwave Technology*, Vol. 25, No. 1, (Jan. 2007), (103–108), ISSN 0733-8724.

Manning, R.J.; Yang, X; Webb, R.P.; Giller, R.; Garcia Gunning, F.C. & Ellis, A.D. (2006). The "turbo-switch" a novel technique to increase the high-speed response of SOAs for wavelength conversion. *Proceedings of OFC/NFOEC*, paper OWS8, Anaheim, USA, Mar. 2006, Optical Society of America.

Matsumoto, A.; Nishimura, K.; Utaka, K. & Usami, M. (2006). Operational design on high-speed semiconductor optical amplifier with assist light for application to wavelength converters using cross-phase modulation. *IEEE J Quantum Electronics*, Vol. 42, No. 3, (Mar. 2006), (313-323), ISSN 0018-9197.

Nakamura, S.; Ueno, Y. & Tajima, K. (2001). 168-Gb/s all-optical wavelength conversion with a symmetric Mach-Zehnder-type switch. *IEEE Photon. Technol. Lett.*, Vol. 13, No. 10, (Oct. 2001), (1091–1093), ISSN 1041- 1135.

Politi, C.; Klonidis, D. & O'Mahony, M.J. (2006). Dynamic behavior of wavelength converters based on FWM in SOAs. *IEEE J Quantum Electronics*, Vol. 42, No. 2, (Feb. 2006), (108-125), ISSN 0018-9197.

Simon, J.C.; Doussiere, P.; Pophillat, L. & Fernier, B. (1989). Gain and noise characteristics of a 1.5 μm near-travelling-wave semiconductor laser amplifier. *J Electronics Letters*, Vol. 25, No. 7, (1989), (434–436), ISSN 0013- 5194.

Tzanakaki, A. & O'Mahony, M.J. (2000). Analysis of tunable wavelength converters based on cross-gain modulation in semiconductor optical amplifiers operating in the

counter propagating mode, *Proceedings of IEE Optoelectronics*, Vol. 147, No. 1, pp. 49–55, Feb. 2000, Institution of Electrical Engineers.

Wei, C.C.; Huang, M.F. & Chen, J. (2005). Enhancing the frequency response of cross-polarization wavelength conversion. *IEEE Photon. Technol. Lett.*, Vol. 17, No. 8, (Aug. 2005), (1683-1685), ISSN 1041-1135.

IntechOpen

IntechOpen

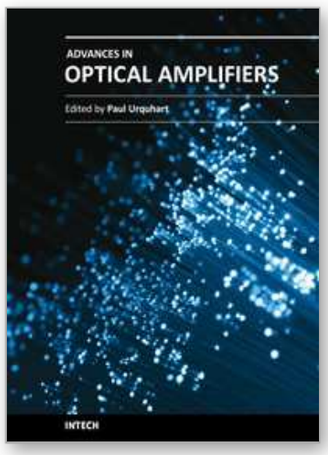

Advances in Optical Amplifiers
Edited by Prof. Paul Urquhart

ISBN 978-953-307-186-2
Hard cover, 436 pages
Publisher InTech
Published online 14, February, 2011
Published in print edition February, 2011

Optical amplifiers play a central role in all categories of fibre communications systems and networks. By compensating for the losses exerted by the transmission medium and the components through which the signals pass, they reduce the need for expensive and slow optical-electrical-optical conversion. The photonic gain media, which are normally based on glass- or semiconductor-based waveguides, can amplify many high speed wavelength division multiplexed channels simultaneously. Recent research has also concentrated on wavelength conversion, switching, demultiplexing in the time domain and other enhanced functions. Advances in Optical Amplifiers presents up to date results on amplifier performance, along with explanations of their relevance, from leading researchers in the field. Its chapters cover amplifiers based on rare earth doped fibres and waveguides, stimulated Raman scattering, nonlinear parametric processes and semiconductor media. Wavelength conversion and other enhanced signal processing functions are also considered in depth. This book is targeted at research, development and design engineers from teams in manufacturing industry, academia and telecommunications service operators.

How to reference
In order to correctly reference this scholarly work, feel free to copy and paste the following:

Youssef Said and Houria Rezig (2011). Semiconductor Optical Amplifier Nonlinearities and Their Applications for Next Generation of Optical Networks, Advances in Optical Amplifiers, Prof. Paul Urquhart (Ed.), ISBN: 978-953-307-186-2, InTech, Available from: http://www.intechopen.com/books/advances-in-optical-amplifiers/semiconductor-optical-amplifier-nonlinearities-and-their-applications-for-next-generation-of-optical

INTECH
open science | open minds

InTech Europe
University Campus STeP Ri
Slavka Krautzeka 83/A
51000 Rijeka, Croatia
Phone: +385 (51) 770 447
Fax: +385 (51) 686 166
www.intechopen.com

InTech China
Unit 405, Office Block, Hotel Equatorial Shanghai
No.65, Yan An Road (West), Shanghai, 200040, China
中国上海市延安西路65号上海国际贵都大饭店办公楼405单元
Phone: +86-21-62489820
Fax: +86-21-62489821

© 2011 The Author(s). Licensee IntechOpen. This chapter is distributed under the terms of the Creative Commons Attribution-NonCommercial-ShareAlike-3.0 License, which permits use, distribution and reproduction for non-commercial purposes, provided the original is properly cited and derivative works building on this content are distributed under the same license.

IntechOpen

IntechOpen